$T$ data obtained from separate simulations. The source of the exponents $A$ and $B$ is not clear, but implications can be drawn from their relative magnitudes. As $A > B$, the separation between the onset and the curve $F = 1$ should diminish as the driving period grows. This means that for long periods, stripes should give way to square or other regular cellular patterns, whereas for shorter periods, irregular structures should dominate.

The significance of dissipation on pattern selection has been commented on previously[9,21]. For example, it has been observed that stripes are present only in high-density, high-dissipation experiments; similar results are obtained in fluids experiments[29,30]. My simulations are consistent with these results: I find that the transition between stripes and square moves closer to onset and then vanishes altogether, as the density, $\rho$, is decreased below $\rho \approx 3$ (measured in units of total particle area divided by available area).

In addition, we see very different densities and dissipation rates for patterned states on opposite sides of the curve $F = 1$. Figure 3 shows representative densities for nearby striped and square patterns. Particles in the square pattern are much more strongly clustered around the vertices, with maximum densities an order of magnitude larger than in the striped pattern. The energies dissipated are very different as well: the mean kinetic energy at the conclusion of a cycle is 270% higher for the square than for the striped pattern.

In conclusion, it may on the one hand seem surprising that an exceedingly simplified model, containing little more than a combination of periodic randomization and dissipation, and entirely neglecting gravity, can produce an apparent wealth of spontaneously organized and highly structured patterns. On the other hand, at a fundamental level there is little difference between this construction and well-known reaction–diffusion models[31,32]. There, too, randomization (in the form of diffusion) competes with dissipation (in the form of reactions) to produce a rich tapestry of regular and irregular patterns. Future experiments may clarify connections between granular and other pattern formation mechanisms. □

Received 18 April; accepted 22 July 1997.


1. Jaeger, H. M., Nagel, S. R. & Behringer, R. P. Granular solids, liquids and gases. *Rev. Mod. Phys.* **68,** 1259–1273 (1996).
2. Ennis, B. J., Green, J. & Davies, R. The legacy of neglect in the US. *Chem. Eng. Progr.* **90,** 32–43 (1994).
3. Ottino, J. M. & Shinbrot, T. Comparing extremes: mixing of fluids, mixing of solids. *NATO-ASI Mixing: Chaos and Turbulence Proc.* (in the press).
4. Metcalf, G., Shinbrot, T., McCarthy, J. J. & Ottino, J. M. Avalanche mixing of granular solids. *Nature* **374,** 39–41 (1995).
5. Hill, K. M. & Kakalios, J. Reversible axial segregation of binary mixtures of granular materials. *Phys. Rev. E* **49,** R3610–R3614 (1994).
6. Bagnold, R. A. The shearing and dilatation of dry sand and the 'singing' mechanism. *Proc. R. Soc. Lond. A* **295,** 219–232 (1966).
7. Nasuno, S., Kudrolli, A. & Gollub, J. P. Friction in granular layers: hysteresis and precursors. *Phys. Rev. Lett.* **79,** 944–952 (1997).
8. Miller, B., O'Hern, C. & Behringer, R. P. Stress fluctuations for continuously sheared granular materials. *Phys. Rev. Lett.* **77,** 3110–3113 (1996).
9. Umbanhowar, P. B., Melo, F. & Swinney, H. L. Localized excitations in a vertically vibrated granular layer. *Nature* **382,** 793–796 (1996).
10. Luding, S., Clément, E., Blumen, A., Rajchenbach, J. & Duran, J. Studies of columns of beads under external vibrations. *Phys. Rev. E* **49,** 1634–1610 (1994).
11. Clément, E., Vanel, L., Rajchenbach, J. & Duran, J. Pattern formation in a vibrated granular layer. *Phys. Rev. E* **53,** 2972–2979 (1996).
12. Pak, H., van Doorn, E. & Behringer, R. Effects of ambient gases on granular materials under vertical vibration. *Phys. Rev. Lett.* **74,** 4643–4647 (1995).
13. Metcalf, T. H., Knight, J. B. & Jaeger, H. M. Standing wave patterns in shallow beds of vibrated granular material. *Physica A* **236,** 202–210 (1997).
14. Melo, F., Umbanhowar, P. & Swinney, H. L. Transition to parametric wave patterns in a vertically oscillated granular layer. *Phys. Rev. Lett.* **72,** 172–175 (1994).
15. Douady, S., Fauve, S. & Laroche, C. Subharmonic instabilities and defects in a granular layer under vertical vibrations. *Europhys. Lett.* **8,** 621–627 (1989).
16. Wassgren, C. R., Brennen, C. E. & Hunt, M. L. Vertical vibration of a deep bed of granular material in a container. *J. Appl. Mech.* **63,** 712–719 (1996).
17. Melo, F., Umbanhowar, P. B. & Swinney, H. L. Hexagons, kinks, and disorder in oscillated granular layers. *Phys. Rev. Lett.* **75,** 3838–3841 (1995).
18. Cerda, E., Melo, F. & Rica, S. A model for parametric waves in granular materials (preprint). (Dept. de Física, Univ. de Santiago, 1997).
19. Luding, S., Clément, E., Rajchenbach, J. & Duran, J. Simulations of pattern formation in vibrated granular media. *Europhys. Lett.* **36,** 247–251 (1996).
20. Menon, N. & Durian, D. J. Diffusing-wave spectroscopy of dynamics in a three-dimensional granular flow. *Science* **275,** 1920–1922 (1997).
21. Metcalf, T. H., Knight, J. B. & Jaeger, H. M. Standing wave patterns in shallow beds of vibrated granular material. *Physica A* **236,** 202–210 (1997).
22. Crawford, J. D., Gollub, J. P. & Lane, D. Hidden symmetries of parametrically forced waves. *Nonlinearity* **6,** 119–164 (1993).
23. Sinai, Ya. G. Dynamical systems with elastic reflections: ergodic properties of dispersing billiards. *Russ. Math. Surv.* **25,** 137–147 (1970).
24. Bleher, S., Grebogi, C. & Ott, E. Bifurcation to chaotic scattering. *Physica D* **46,** 87–121 (1990).
25. Chen, Q., Ding, M.-Z. & Ott, E. Chaotic scattering in several dimensions. *Phys. Lett. A* **115,** 93–95 (1990).
26. Ding, M.-Z., Grebogi, C., Ott, E. & Yorke, J. A. Transition to chaotic scattering. *Phys. Rev. A* **42,** 7025–7040 (1990).
27. Bizon, C., Shattuck, M. D., Swift, J. B., McCormick, W. D. & Swinney, H. L. Patterns in 3D vertically oscillated granular layers: simulation and experiment. *Phys. Rev. Lett.* (in the press).
28. Tsimring, L. & Aranson, I. Localized and cellular patterns in a vibrated granular layer. *Phys. Rev. Lett.* **79,** 213–216 (1997).
29. Kudrolli, A. & Gollub, J. P. Localized spatiotemporal chaos in surface waves. *Phys. Rev. E* **54,** R1052–R1055 (1996).
30. Edwards, W. & Fauve, S. Patterns and quasi-patterns in the Faraday experiment. *J. Fluid Mech.* **278,** 123–134 (1994).
31. Winfree, A. T. Spiral waves of chemical activity. *Science* **175,** 634–638 (1972).
32. Pearson, J. E. Complex patterns in a simple system. *Science* **261,** 189–192 (1993).


**Acknowledgements.** I thank J. M. Ottino for thoughtful advice, J. J. McCarthy for valuable comments and assistance, and H. Jaeger, M. Mavrovouniotis, H. Swinney and P. Umbanhowar for crucial scientific discussions. This work was supported by the National Science Foundation (Division of Chemical and Transport Systems) and the American Chemical Society (Petroleum Research Fund).

Correspondence and requests for materials should be addressed to the author (e-mail: shinbrot@nwu.edu).

# Induced long-range order in crosslinked 'one-dimensional' stacks of fluid monolayers

**Gerald C. L. Wong*, Wim H. de Jeu*, Henry Shao†, Keng S. Liang† & Rudolf Zentel‡**

* *FOM Institute for Atomic and Molecular Physics, Kruislaan 407, 1098SJ Amsterdam, The Netherlands*
† *Exxon Research and Engineering Company, Annandale, New Jersey 08801, USA*
‡ *Fachbereich 9: Chemie und Biologie, Bergische Universität Wuppertal, Gauss-Strasse 20, D-42097 Wuppertal, Germany*

**Ordinary crystals are characterized by long-range translational order in all three dimensions. In lower-dimensional systems, in contrast, translational order is destroyed through the 'Landau–Peierls instability'—displacements from periodic ordering due to thermal fluctuations whose amplitude increases with the size of the system[1–4]. This effect is well known for layered systems ordered in one dimension, such as surfactant membranes[5,6], smectic (layered) liquid crystals[7] and liquid crystalline polymers[8], which form ordered stacks of fluid monolayers. Smectic liquid-crystal polymers can be weakly crosslinked to form percolating elastomeric networks that still allow mobility on a molecular scale[9,10]. In these smectic elastomers, fluctuations of the fluid layers are coupled to distortions of the underlying network, and are therefore energetically penalized[11], even though the network of crosslinks has a random nature and thus no three-dimensional translational order. Here we present a high-resolution X-ray diffraction study of a smectic elastomer that reveals the effects of crosslinking on long-range ordering. We find that the introduction of a random network of crosslinks enhances the stability of the layered structure against thermal fluctuations and suppresses the Landau–Peierls instability so as to induce 'one-dimensional' long-range ordering at length-scales up to several micrometres.**

Landau[1] and Peierls[2] were the first to demonstrate that translational order is destroyed in one- and two-dimensional systems by thermal fluctuations. In three-dimensional space similar arguments can be applied to, for example, a smectic system of stacked fluid monolayers, where rod-like mesogenic (liquid-crystal-forming) molecules order into a 'one-dimensional' density wave along one direction, but remain fluid in the other two (Fig. 1a). In such a system the mean squared layer displacement diverges logarith-

mically with the system size at all finite temperatures ('Landau–Peierls instability'). The resultant X-ray diffraction signature has been calculated by Caillé[12]. In the direction perpendicular to the layers, these divergent thermal fluctuations transform the discrete Bragg peaks (indicative of translational order) into algebraic 'cusps' with the structure factor $S$ having an asymptotic power-law form:

$$S(0, 0, q_z) \approx \frac{1}{|q_z - q_m|^{2-\eta_m}}$$

where $q_z$ represents the wave vector transfer along the density wave, $q_m$ represents the position of the $m$th order of diffraction ($q_m = mq_0$, $q_0 = 2\pi/d$, $m = 1, 2, 3, \ldots$, and $d$ is the smectic layer spacing). The exponent $\eta_m$ is given by $\eta_m = q_m^2 k_B T/(8\pi(BK)^{\frac{1}{2}})$ and directly related to the elastic constants of this smectic system: $K$ is the bending modulus and $B$ is the layer compression modulus ($T$ is temperature, and $k_B$ is Boltzmann's constant). The magnitude of $\eta_m$ is quite small, with typical measured values of ~0.1–0.3 near the smectic-A/nematic phase transition temperature ($T_{AN}$), where $B$ approaches zero. At all other temperatures, $\eta_m \approx 0$, which results in a saturated lineshape with 'tails' given by $1/q^2$. This can make the discrimination between Caillé lineshapes and normal Bragg peaks difficult, as Bragg peaks broaden into an asymptotic $1/q^2$ form as well, due to contributions from dynamical effects and thermal diffuse scattering[13].

In a smectic polymer (Fig. 1b) the mesogenic molecules are attached to polymer chains via flexible spacer groups. Although the phase transition temperatures can differ significantly from those of its monomeric counterpart due to the coupling between the 'one-dimensional' layering and the three-dimensional ensemble of polymer chains, the Landau–Peierls instability persists in such smectic polymers: the Bragg peaks are still destroyed by fluctuations[8]. These liquid-crystalline polymers can be weakly crosslinked into an elastomer network (Fig. 1c) with almost no change in the phase transition temperatures. The macroscopic rubber elasticity introduced via such a network[14] interacts with the liquid crystalline ordering. In the case of nematic elastomer networks, where the mesogenic units are aligned but not layered, novel forms of mechanical instabilities and orientational memory effects have been observed[15]. In a smectic elastomer, the fluctuating smectic layers cannot move past crosslinks in the network: this network coupling imposes a penalty for relative translations between the orientationally ordered fluid layers and the polymer network. A recent continuum theory has predicted that the fluctuations associated with the Landau–Peierls instability can be suppressed in a smectic elastomer, so that the usual logarithmic divergence of the mean squared layer displacements no longer exists[11]. The marginally stable, quasi-periodic structure of normal 'one-dimensional' fluid stacks should be transformed into a fully periodic structure with proper long-range order, and the resultant diffraction should change from Caillé lineshapes to normal Bragg peaks.

A smectic elastomer system has a significant degree of random disorder, which is not included in the original theoretical model (ref. 11). When such a random field is taken into account the quenched static disorder will eventually destroy translational long-range order at large length-scales (small $q$ values), so that the discrimination between Bragg peaks and Caillé lineshapes must be made at large enough $q$ values. We note that the Caillé lineshape cannot have an asymptotic $q$-dependence that is steeper than $1/q^2$, whereas the behaviour of a true Bragg peak is not bound by this constraint. Even a Bragg peak that has been broadened by lattice imperfections[16] can in principle still be sharper than $1/q^2$, and may not reach this asymptotic limit for several decades of intensity.

The basic macromolecular system used in this study is a smectic random copolymer with a comb-like architecture[17]. Most of the side chains connect rigid 'rod-like' molecules to the polyacrylate backbone, which provide the system with liquid crystalline phase behaviour (Fig. 2). A small fraction (~5%) of the side-chains, however, terminate with functional hydroxyl groups, and serve as active sites for the crosslinking process. These 'linear' liquid-crystalline copolymer chains can be transformed into a weakly linked, 'infinite-molecular-weight' network via reaction with a crosslinking agent in a solvent (Fig. 1c and Fig. 2). The measurements reported below were performed at beamline X-10A of the National Synchrotron Light Source, Brookhaven National Laboratory, USA. To get monodomain samples, the uncrosslinked polymer is aligned with a magnetic field in a temperature-controlled cell. In contrast, the liquid-crystalline groups in the crosslinked elastomer are aligned with a strain field, which is applied *in situ* to freely suspended samples in a different temperature-controlled cell with an internal translation stage. Owing to the multiple-Bragg reflections in the monochromator and the analyser crystals, the measured intensity of the incident beam has an approximately $1/q^{3.6}$ dependence, which is much sharper than $1/q^2$ and therefore sufficiently steep for the present lineshape measurement. The in-plane liquid-like disorder has been independently confirmed by wide-angle X-ray scattering.

Measurements for both the uncrosslinked smectic polymer and the crosslinked smectic elastomer were done at $T = 55.0\,^\circ$, which is in the smectic-A phase well below $T_{AN}$ and well above the glass transition temperature $T_g$. The full mosaic width, which measures the variation of layering directions about the average, is 2.5° for the elastomer and 4.1° for the polymer. Figure 3a shows the scattering intensity from the first-order diffraction of the aligned elastomer. The scattering intensity for the smectic elastomer decreases rapidly away from $q_1$, with a slope of $-2.40 \pm 0.10$ on a log–log plot over three orders of magnitude. The Bragg scattering from the elastomer is significantly sharper than a Caillé power-law lineshape, which saturates at a limiting slope of −2 at these temperatures. Figure 3b compares the asymptotic slopes of the diffuse scattering from the crosslinked elastomer and the corresponding uncrosslinked polymer. The dramatic sharpening of the elastomer lineshape is correlated with the existence of percolating crosslinks and the resultant change in polymer topology. In contrast to the lineshape of the

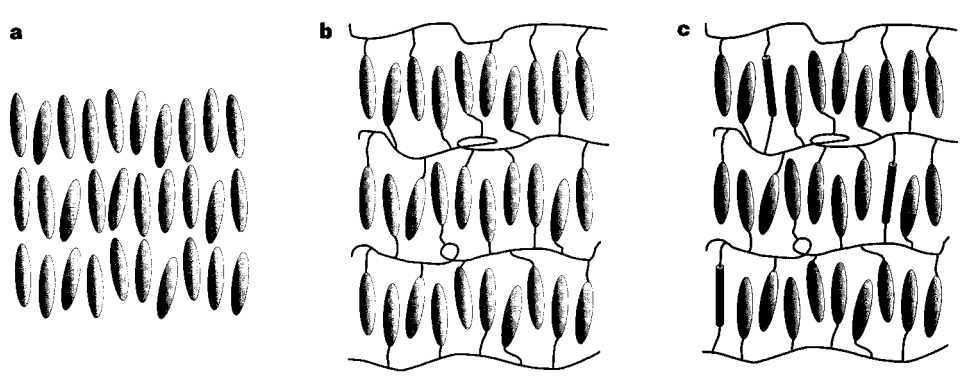


**Figure 1** Schematic representation of a smectic liquid crystal (**a**), a smectic-crystalline polymer (**b**), and a weakly crosslinked smectic elastomer network (**c**). Crosslinks are represented by cylinders. The low density of crosslinks provides the smectic elastomer system with solid-like behaviour at macroscopic length-scales while retaining liquid-like behaviour at microscopic length-scales.

elastomer, the intensity tails of the uncrosslinked polymer have a slope of $-1.85 \pm 0.10$. The absolute value of the measured slope is expected to be somewhat less than the theoretical limit of 2 owing to the finite mosaic width of the sample. In fact, the mosaic distribution causes the Caillé lineshape to vary continuously between a power law with an exponent of $2 - \eta_m$ (for a single-orientation sample with no mosaic spread) to one with an exponent of $1 - \eta_m$ (for a random powder)[18]. Moreover, we have performed measurements on a sample of the same compound with a narrower mosaic width, which is possible at temperatures closer to $T_{AN}$, and obtained the established saturation value of –2 for the asymptotic slope.

We emphasize that the smectic elastomer network remains liquid at microscopic length-scales, even though it is a soft solid at macroscopic length-scales. Macroscopic deformations of the sample were found to drastically change the orientational distribution and layering texture at the molecular level. This is also evident in preliminary measurements of the weak higher-order diffraction (data not shown), which is sensitive to the 'sharpness' of layer interfaces at length-scales smaller than a smectic layer spacing, and is therefore susceptible to such liquid-like disorder. More importantly, the sample can melt into its nematic and isotropic phases on heating and reorder into the present rubber-like smectic phase. In other words, the smectic elastomer forms a soft, thermodynamically stable 'one-dimensional' lattice, and not a quenched 'glassy' solid with frozen-in order. In addition, the characteristic timescale that separates solid-like behaviour and liquid-like behaviour decreases as $T_{AN}$ is approached from lower temperatures. Consequently the dynamical coupling responsible for the suppression of the Landau–Peierls instability is expected to disappear near $T_{AN}$ (ref. 19).

Owing to its random nature, the elastomer lattice is expected to

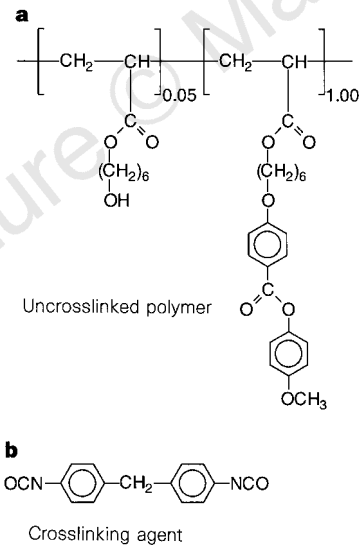


**Figure 2** The polymer and crosslinking agent used in these experiments. **a**, The uncrosslinked polyacrylate-based, side-chain liquid-crystalline polymer (number-average relative molecular mass, 11,200), synthesized by radical copolymerization. The proportion of side-chains which terminate with functional hydroxyl groups is 5 mol.%. **b**, Crosslinking is achieved by reaction with 4,4′-diphenylmethane di-isocyanate under basic conditions (triethylamine) in toluene. The similarity in the phase sequences of the elastomer (g 31 $S_A$ 80 N 111 I) and the uncrosslinked polymer (g 26 $S_A$ 82 N 110 I) has been verified with differential scanning calorimetry and polarizing microscopy (temperatures given in °C; g, $S_A$ and N indicate the glassy, smectic-A and nematic phases, respectively). The crosslink density of the smectic elastomer network is ~2–5 mol.%, as estimated from a swelling experiment in toluene.

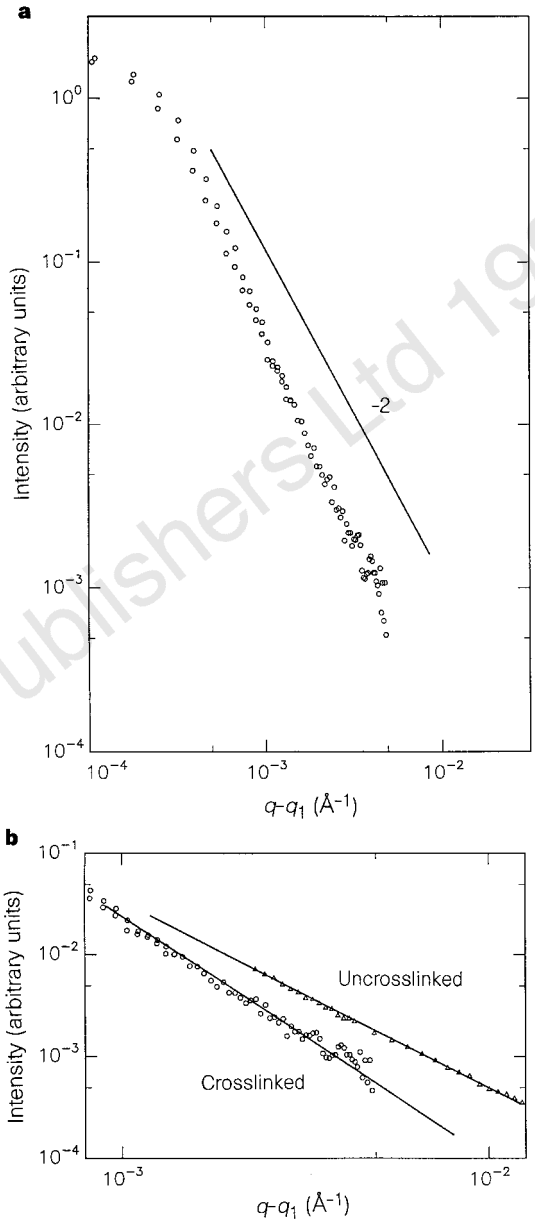


**Figure 3** Results of X-ray diffraction studies. **a**, A log–log plot of the background-subtracted first-order diffraction intensity from the smectic elastomer network. The diffraction intensity decreases sharply away from $q_1$ and is significantly sharper than the normal Caillé lineshape for stacked fluid layers (limiting slope, –2). **b**, Comparison of the asymptotic diffraction intensity tails from the elastomer (circles; $q_1 = 0.255$ Å$^{-1}$, slope of $2.40 \pm 0.10$) and the corresponding uncrosslinked polymer (triangles; $q_1 = 0.253$ Å$^{-1}$, slope of $1.85 \pm 0.10$). The sharpening of the elastomer lineshape is clearly associated with the existence of crosslinks. The asymptotic slope is reached at slightly different $q$ ranges for the two samples owing to domain size effects. The uncrosslinked polymer was sealed in a quartz capillary (1.5 mm diameter), and placed between the poles of a 0.8 T $SmCo_5$ magnet, inside the inner stage of a two-stage sample cell with a temperature stability of ±30 mK. Alignment of the smectic planes in the uncrosslinked polymer was achieved by cooling the sample from the nematic phase at $T = 100$ °C in the magnetic field, at a rate of 0.2 °C h$^{-1}$. The elastomer sample (~7 × 2 × 1 mm) was stretched *in situ* by 25% in the nematic phase at 90 °C, then subsequently cooled into an aligned smectic phase. The sample cells were coupled to a 4-circle diffractometer, with $q_z$ orientated perpendicular to the smectic layers. The monochromator and the analyser consisted of a double-bounce Si(111) and a triple-bounce Ge(111) channel-cut crystal set non-dispersively at a wavelength of $\lambda = 1.5347$ Å, which resulted in a sharp in-phase resolution of $\Delta q_z = 1.6 \times 10^{-4}$ Å$^{-1}$, given by the half-width at half-maximum of the incident beam.

have a high density of defects. It is interesting to compare these defects with flux vortex lattices in superconductivity[20]. At large enough length-scales (above the so-called Larkin length), even arbitrarily weak static defects can destroy translational long-range order for all dimensions $< 4$. For flux vortex lattices, the defects are rigidly fixed in space, and not connected to the fluctuating lattice. Long-range order is therefore always destroyed at large enough length-scales. The analogy with smectic elastomers is complex, because the defects are crosslinks which are embedded in the fluctuating lattice itself, and therefore are not strictly static. We observed $1/q^{2.4}$ intensity tails which persist down to $q$ values approaching our experimental resolution limit, which is high enough to resolve length-scales of several micrometres. For the limiting case of static crosslinks, the scattering signature may consist of a crossover between the disordered Larkin limit at a small $q$, to the predicted Bragg behaviour at large $q$, which is the range we observe. As the Larkin length has been known to be macroscopically large even for soft lattices (tens of micrometres) we may not be able to observe this effect even at the high resolution of our experiments. But because crosslinks can locally disturb the smectic layering, and can even destroy the 'one-dimensional' lattice down to molecular length-scales at high crosslink densities[21], the lineshape at our measured range of $q$ values can also be affected. As with effects related to the mosaic width, such defects can only broaden rather than sharpen the lineshape associated with the 'one-dimensional' ordering, and therefore cannot explain our unambiguous observation of an elastomer Bragg peak that is sharper than the Caillé lineshape. In these smectic elastomers the introduction of disorder in the form of a random network has the counterintuitive result of enhancing the 'one-dimensional' ordering. □

Received 29 November 1996; accepted 15 August 1997.


1. Landau, L. D. in *Collected Papers of L. D. Landau* (ed. ter Haar, D.) 193–216 (Gordon & Breach, New York, 1965).
2. Peierls, R. E. Bemerkung über Umwandlungstemperaturen. *Helv. Phys. Acta Suppl.* **7,** S81–S83 (1934).
3. Chaikin, P. M. & Lubensky, T. C. *Principles of Condensed Matter Physics* (Cambridge Univ. Press, New York, 1995).
4. de Gennes, P. G. & Prost, J. *The Physics of Liquid Crystals* 2nd edn (Clarendon Press, Oxford, 1993).
5. Safinya, C. R. *et al*. Steric interactions in a model multimembrane system: a synchrotron X-ray study. *Phys. Rev. Lett.* **57,** 2718–2721 (1986).
6. Sirota, E., Smith, G. S., Safinya, C. R., Plano, R. J. & Clark, N. A. X-ray scattering studies of aligned, stacked surfactant membranes. *Science* **242,** 1406–1409 (1988).
7. Als-Nielsen, J. *et al*. Observation of algebraic decay of positional order in a smectic liquid crystal. *Phys. Rev.* **B22,** 312–320 (1980).
8. Nachaliel, E., Keller, E. N., Davidov, D. & Boeffel, C. Algebraic dependence of the structure factor and possible anharmonicity in a high resolution X-ray study of a side-group polymeric liquid crystal. *Phys. Rev.* **A43,** 2897–2902 (1991).
9. Zentel, R. Liquid crystalline elastomers. *Angew. Chem. Adv. Mater.* **101,** 1407–1415 (1989).
10. Finkelmann, H., Benne, J. & Semmler, K. Smectic liquid crystal elastomers. *Macromol. Symp.* **96,** 169–174 (1995).
11. Terentjev, E. M., Warner, M. & Lubensky, T. C. Fluctuations and long-range order in smectic elastomers. *Europhys. Lett.* **30,** 343–348 (1995).
12. Caillé, A. Remarques sur la diffusion des rayons X dans les smectiques. *C. R. Acad. Sci. Paris* **B274,** 891–893 (1972).
13. Warren, B. E. *X-ray Diffraction* (Addison-Wesley, Reading, 1969).
14. de Gennes, P. G. in *Polymer Liquid Crystals* (eds Ciferri, A., Krigbaum, W. R. & Meyer, R. B.) 115–132 (Academic, New York, 1982).
15. Mitchell, G. R., Davis, F. J. & Guo, W. Strain-induced transitions in liquid-crystal elastomers. *Phys. Rev. Lett.* **71,** 2947–2950 (1993).
16. Krivoglaz, M. *Theory of X-ray and Thermal Neutron Scattering by Real Crystals* (Plenum, New York, 1969).
17. Zentel, R. & Benalia, M. Stress-induced orientation in lightly crosslinked liquid-crystalline side-group polymers. *Makromol. Chem.* **188,** 665–674 (1987).
18. Kaganer, V. M., Ostrovsky, B. I. & de Jeu, W. H. X-ray scattering in smectic liquid crystals: from ideal- to real-structure effects. *Phys. Rev.* **A44,** 8158–8166 (1991).
19. Olmsted, P. D. & Terentjev, E. M. Mean-field nematic-smectic-A transition in a random polymer network. *Phys. Rev.* **E53,** 2444–2453 (1996).
20. Blatter, G., Feigelíman, M. V., Geshkenbein, V. B., Larkin, A. I. & Vinokur, V. M. Vortices in high temperature superconductors. *Rev. Mod. Phys.* **66,** 1125–1380 (1994).
21. Terentjev, E. M. Non-uniform deformations and molecular random fields in liquid crystalline elastomers. *Macromol. Symp.* **117,** 79–88 (1997).


**Acknowledgements.** We thank E. M. Terentjev for discussions, E. Gebhard for assistance in sample preparation, and J. Commandeur for technical support. This work is part of the research program of the Stichting voor Fundamenteel Onderzoek der Materie [Foundation for Fundamental Research on Matter (FOM)] with support from the Nederlandse Organisatie voor Wetenschappelijk Onderzoek [Netherlands Organization for the Advancement of Research (NWO)]. W.d.J. acknowledges additional support from a NATO collaborative research grant.

Correspondence and requests for materials should be addressed to W.H.d.J. (e-mail: dejeu@amolf.nl)

# Origin of rubber-like behaviour in metal alloys

**Xiaobing Ren & Kazuhiro Otsuka**

*Institute of Materials Science, University of Tsukuba, Tsukuba, Ibaraki 305, Japan*

**Since 1932 it has been known that a number of ordered alloys show an unusual kind of deformation behaviour[1–3]. These alloys (including Au–Cd, Au–Cu–Zn, Cu–Zn–Al, Cu–Al–Ni)[4–8], after being aged for some time in a martensitic state (the low-symmetry phase of a diffusionless transformation), can be deformed like a soft and pseudo-elastic rubber (with a recoverable strain as large as a few per cent). Accompanying martensite ageing is the development of martensite stabilization[9] (increase in the temperature of reverse transformation to the parent state), the avoidance of which is important in actuator applications of the shape-memory effect[29], (which these alloys also generally exhibit. The origin of this rubber-like behaviour and of the ageing effect has remained unclear[10–17]. Here we show that this behaviour does not involve a change in the degree of long-range order, but is instead due to an atomic rearrangement within the same sublattice of the imperfectly ordered alloy during martensite ageing. This process is driven by a general tendency for the equilibrium symmetry of the short-range order configuration of lattice imperfections to conform to the symmetry of the lattice. This principle not only explains all the observed aspects of the rubber-like behaviour and the ageing effect in both ordered and disordered alloys, but may also further our understanding of some diffusion phenomena in other crystalline materials.**

A martensitic transformation lowers the symmetry of a crystal without involving atomic exchange or diffusion. As a result of symmetry lowering, a single crystal of the parent phase (high-temperature phase) is split into many twin-related martensite domains. If the martensite of the above-mentioned alloys is deformed immediately after being transformed from the parent phase, the strain can be accommodated by the easy reversal of some of the domains into new ones, that is, twinning. This explains the 'softness' of the martensite. Because the stress-induced domains have the same martensite structure and hence the same stability as

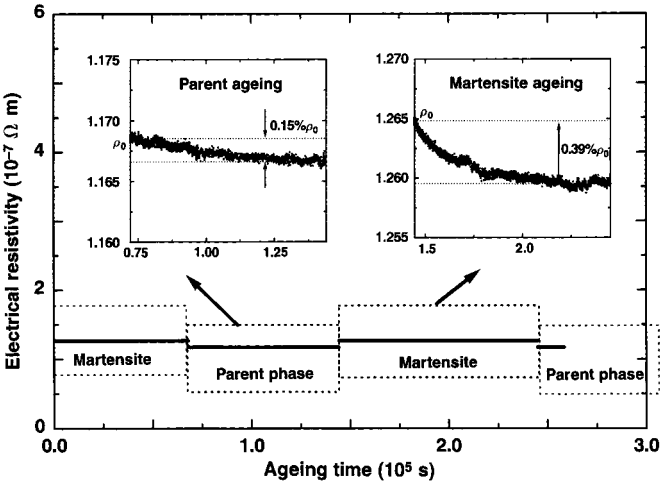


**Figure 1** Electrical resistivity of single crystal $Au_{50.5}Cd_{49.5}$ alloy as a function of ageing time, for the parent phase (enlarged in the left inset) after transformation from well-aged martensite, and for martensite (enlarged in the right inset) after transformation from well-aged parent.